How to compare adversarial robustness of classifiers from a global perspective

Niklas Risse*   Christina Göpfert*   Jan Philip Göpfert*

Bielefeld University, Germany

Abstract

Adversarial robustness of machine learning models has attracted considerable attention over recent years. Adversarial attacks undermine the reliability of and trust in machine learning models, but the construction of more robust models hinges on a rigorous understanding of adversarial robustness as a property of a given model. Point-wise measures for specific threat models are currently the most popular tool for comparing the robustness of classifiers and are used in most recent publications on adversarial robustness. In this work, we use recently proposed robustness curves to show that point-wise measures fail to capture important global properties that are essential to reliably compare the robustness of different classifiers. We introduce new ways in which robustness curves can be used to systematically uncover these properties and provide concrete recommendations for researchers and practitioners when assessing and comparing the robustness of trained models. Furthermore, we characterize scale as a way to distinguish small and large perturbations, and relate it to inherent properties of data sets, demonstrating that robustness thresholds must be chosen accordingly. We release code to reproduce all experiments presented in this paper, which includes a Python module to calculate robustness curves for arbitrary data sets and classifiers, supporting a number of frameworks, including TensorFlow, PyTorch and JAX.

1 Introduction

Despite their astonishing success in a wide range of classification tasks, deep neural networks can be lead to incorrectly classify inputs altered with specially crafted adversarial perturbations [35, 11]. These perturbations can be so small that they remain almost imperceptible to human observers [13]. Adversarial robustness describes a model's ability to behave correctly under such small perturbations crafted with the intent to mislead the model. The study of adversarial robustness – with its definitions, their implications, attacks, and defenses – has attracted considerable research interest. This is due to both the practical importance of trustworthy models as well as the intellectual interest in the differences between decisions of machine learning models and our human perception. A crucial starting point for any such analysis is the definition of what exactly a small input perturbation is – requiring (a) the choice of a *distance function* to measure perturbation size, and (b) the choice of a particular *scale* to distinguish small and large perturbations. Together, these two choices determine a *threat model* that defines exactly under which perturbations a model is required to be robust.

The most popular choice of distance function is the class of distances induced by ℓ_p norms [35, 11, 6], in particular ℓ_1, ℓ_2 and ℓ_∞, although other choices such as Wasserstein distance have been explored as well [40]. Regarding scale, the current default is to pick some perturbation threshold ε without providing concrete reasons for the exact choice. Analysis then focuses on the *robust error* of the model, the proportion of test inputs for which the model behaves incorrectly under some perturbation up to size ε. This means that the scale is defined as a binary distinction between small and large perturbations based on the perturbation threshold. A set of canonical thresholds have emerged in the

literature. For example, in the publications referenced in this section, the `MNIST` data set is typically evaluated at a perturbation threshold $\varepsilon \in \{0.1, 0.3\}$ for the ℓ_∞ norm, while `CIFAR-10` is evaluated at $\varepsilon \in \{2/255, 4/255, 8/255\}$, stemming from the three 8-bit color channels used to represent images.

Based on these established threat models, researchers have developed specialized methods to minimize the robust error during training, which results in more robust models. Popular approaches include specific data augmentation, sometimes used under the umbrella term adversarial training [14, 24, 7, 16], training under regularization that encourages large margins and smooth decision boundaries in the learned model [15, 38, 9, 10], and post-hoc processing or randomized smoothing of predictions in a learned model [20, 8].

In order to show the superiority of a new method, robust accuracies of differently trained models are typically compared for a handful of threat models and data sets, eg., $\ell_\infty(\varepsilon = 0.1)$ and $\ell_2(\varepsilon = 0.3)$ for `MNIST`. Out of 22 publications on adversarial robustness published at NeurIPS 2019, ICLR 2020, and ICML 2020, 12 publications contain results for only a single perturbation threshold. In five publications, robust errors are calculated for at least two different perturbation thresholds, but still, only an arbitrary number of thresholds is considered. Only in five out of the total 22 publications do we find extensive considerations of different perturbation thresholds and the respective robust errors. Out of these five, three are analyses of randomized smoothing, which naturally gives rise to certification radii [22, 7, 29]. Najafi et al. [28] follow a learning-theoretical motivation, which results in an error bound as a function of the perturbation threshold. Only Maini et al. [26] do not rely on randomization

---

*equal contribution

and still provide a complete, empirical analysis of robust error for varying perturbation thresholds[1].

Our contributions: In this work, we demonstrate that point-wise measures of ℓ_p robustness are not sufficient to reliably and meaningfully compare the robustness of different classifiers. We show that, both in theory and practice, results of model comparisons based on point-wise measures may fail to generalize to threat models with even slightly larger or smaller ε and that robustness curves avoid this pitfall by design. Furthermore, we show that point-wise measures are insufficient to meaningfully compare the efficacy of different defense techniques when distance functions are varied, and that robustness curves, again, are able to reliably detect and visualize this property. Finally, we analyze how scale depends on the underlying data space, choice of distance function, and distribution. It is our belief that the continued use of single perturbation thresholds in the adversarial robustness literature is due to a lack of awareness of the shortcomings of these measures. Based on our findings we suggest that robustness curves should become the standard tool when comparing adversarial robustness of classifiers, and that the perturbation threshold of threat models should be selected carefully in order to be meaningful, considering inherent characteristics of the data set. We release code to reproduce all experiments presented in this paper[2], which includes a Python module with an easily accessible interface (similar to Foolbox, Rauber et al. [31]) to calculate robustness curves for arbitrary data sets and classifiers. The module supports classifiers written in most of the popular machine learning frameworks, such as TensorFlow, PyTorch and JAX.

2 Methods

An adversarial perturbation for a classifier f and input-output pair (x, y) is a small perturbation δ with $f(x + \delta) \neq y$. Because the perturbation δ is small, it is assumed that the label y would still be the correct prediction for $x + \delta$. The resulting point $x + \delta$ is called an adversarial example. The points vulnerable to adversarial perturbations are the points that are either already misclassified when unperturbed, or those that lie close to a decision boundary.

One tool to visualize and study the robustness behavior of a classifier are *robustness curves* [12]. A robustness curve captures the distribution of shortest distances between a set of points and the decision boundaries of a classifier:

Definition 1. *Given an input space $\mathcal{X}$ and label set $\mathcal{Y}$, distance function d on $\mathcal{X} \times \mathcal{X}$, and classifier $f : \mathcal{X} \rightarrow \mathcal{Y}$. Assume $(x, y) \sim_{i.i.d.} P$ for some distribution P on $\mathcal{X} \times \mathcal{Y}$. Then the d-robustness curve for f is the graph of the function*

$$R_d^f(\varepsilon) := P\left(\{(x, y) \text{ s.t. } \exists\, x' : d(x, x') \leqslant \varepsilon \wedge f(x') \neq y\}\right)$$

Since a model's robustness curve shows how data points are distributed in relation to the decision boundaries of the model, it

allows us to take a step back from robustness regarding a specific perturbation threshold, and instead allows us to compare global robustness properties and their dependence on a given classifier, distribution and distance function. To see why this is relevant, consider Figure 1, which shows toy data along with two possible classifiers that perfectly separate the data. For a perturbation threshold of ε, the blue classifier has robust error 0.5, while the orange classifier is perfectly robust. However, for a perturbation threshold of 2ε, the orange classifier has robust error 1, while the blue classifier remains at 0.5. By freely choosing a single perturbation threshold for comparison, it is therefore possible to make either classifier appear to be much better than the other, and no single threshold can capture the whole picture. In fact, for any two disjoint sets of perturbation thresholds, it is possible to construct a data distribution and two classifiers f, f', such that the robust error of f is lower than that of f' for all perturbation thresholds in the first set, and that of f' is lower than that of f for all perturbation thresholds in the second set. See Appendix A for a constructive proof.

3 Experiments

In the following, we empirically evaluate the robustness of a number of recently published models, and demonstrate that the weaknesses of point-wise measures described above are not limited to toy examples, but occur for real-world data and models.

3.1 Experimental Setup

We evaluate and compare the robustness of models obtained using the following training methods:

1. Standard training (ST), i.e., training without specific robustness considerations.
2. Adversarial training (AT) [24].
3. Training with robust loss (KW) [38].
4. Maximum margin regularization for a single ℓ_p norm together with adversarial training (MMR + AT) [9].
5. Maximum margin regularization simultaneously for ℓ_∞ and ℓ_1 margins (MMR-UNIV) [10].

Together with each training method, we state the threat model the trained model is optimized to defend against, eg., $\ell_\infty(\varepsilon = 0.1)$ for perturbations in ℓ_∞ norm with perturbation threshold $\varepsilon = 0.1$, if any. The trained models are those made publicly available by Croce et al. [9][3] and Croce and Hein [10][4]. The network architecture is a convolutional network with two convolutional layers, two fully connected layers and ReLU activation functions. The evaluation is based on six real-world datasets: MNIST, Fashion-MNIST (FMNIST) [41], German Traffic Signs (GTS) [17], CIFAR-10 [19], Tiny-Imagenet-200 (TINY-IMG) [23], and Human Activity Recognition (HAR) [2]. For specifics on model training (hyperparameters, architecture details), refer to Appendix C. Models are generally trained on the full training set

---

[1]*Single thresholds:* [27, 36, 1, 4, 30, 37, 34, 10, 42, 32, 43, 33], *multiple thresholds:* [21, 25, 16, 39, 3], *full analysis:* [29, 7, 22, 28, 26].

[2]The full code is available at https://github.com/niklasrisse/how-to-compare-adversarial-robustness-of-classifiers-from-a-global-perspective.

[3]The models trained with ST, KW, AT and MMR + AT are avaible at www.github.com/max-andr/provable-robustness-max-linear-regions.

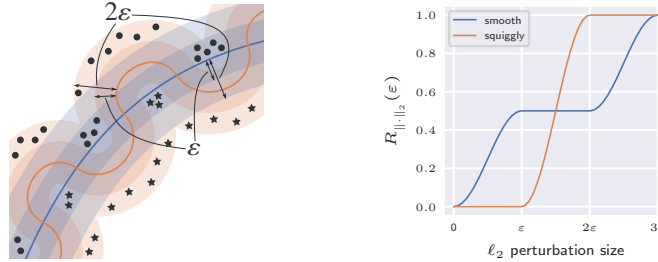[4]The models trained with MMR-UNIV are avaible at www.github.com/fra31/mmr-universal.

Figure 1: Excerpt of a toy data set with two decision boundaries (left) and respective robustness curves (right). The data is separated perfectly by one smooth boundary (blue robustness curve), and one squiggly boundary (orange robustness curve). We indicate margins around the boundaries at distances ε and 2ε. Selecting a single perturbation threshold is not sufficient to decide which classifier is more robust.

for the corresponding data set, and robustness curves evaluated on the full test set, unless stated otherwise.

For complex models, calculating the exact distance of a point to the closest decision boundary, and thus estimating the true robustness curve, is computationally very intensive, if not intractable. Therefore we bound the true robustness curve from below using strong adversarial attacks, which is consistent with the literature on empirical evaluation of adversarial robustness and also applicable to many different types of classifiers. We base our selection of attacks on the recommendations by Carlini et al. [6]. Specifically, we use the ℓ_2-attack proposed by [5] for ℓ_2 robustness curves and PGD [24] for ℓ_∞ robustness curves. For both attacks, we use the implementations of Foolbox [31]. See Appendix C for information on adversarial attack hyperparameters. In the following, "robustness curve" refers to this empirical approximation of the true robustness curve.

3.2 The weaknesses of point-wise measures

Point-wise measures are used to quantify robustness of classifiers by measuring the robust test error for a specific distance function and a perturbation threshold (eg., $\ell_\infty(\varepsilon = 4/255)$). In Table 1 we show three point-wise measures to compare the robustness of five different classifiers on CIFAR-10. If we compare the robustness of the four robust training methods (latter four columns of the table) based on the first point-wise threat model $\ell_\infty(\varepsilon = 1/255)$ (first row of the table), we can see that the classifier trained with AT is the most robust, followed by MMR + AT, followed by KW, and MMR-UNIV results in the least robust classifier. However, if we increase the ε of our threat model to $\varepsilon = 4/255$ (second row of the table), KW is more robust than AT. For a even larger ε (third row of the table), we would conclude that MMR-UNIV is preferable over AT, and that AT results in the least robust classifier. All three statements are true for the particular perturbation threshold (ε), and the magnitude of all perturbation thresholds is reasonable: publications on adversarial robustness typically evaluate CIFAR-10 on perturbation thresholds $\leqslant 10/255$ for ℓ_∞ perturbations. Meaningful conclusions on the robustness of the classifiers relative to each other can not be made without taking all possible ε into account. In other words, a global perspective is needed.

3.2.1 A global perspective

Figure 2 shows the robustness of different classifiers for the ℓ_∞ (right plot) and ℓ_2 (left plot) distance functions from a global perspective using robustness curves. The plot reveals why the three point-wise measures (marked by vertical black dashed lines in the left plot) lead to different results in the relative ranking of robustness of the classifiers. Both for the classifiers trained to be robust against attacks in ℓ_∞ distance (left plot) and ℓ_2 distance (right plot), we can observe multiple intersections of robustness curves, corresponding to changes in the relative ranking of the robustness of the compared classifiers. The robustness curves allow us to reliably compare the robustness of classifiers for all possible perturbation thresholds. Furthermore, the curves clearly show the perturbation threshold intervals with strong and weak robustness for each classifier, and are not biased by an arbitrarily chosen perturbation threshold.

3.2.2 Overfitting to specific perturbation thresholds

In addition to the problem of robustness curve intersection, relying on point-wise robustness measures to evaluate adversarial robustness is prone to overfitting when designing training procedures. Figure 3 shows ℓ_∞ robustness curves for MMR + AT with ℓ_∞ threat model as provided by Croce et al. [9]. The models trained on MNIST and FMNIST both show a change in slope, which could be a sign of overfitting to the specific threat models for which the classifiers were optimized for, since the change of slope occurs approximately at the chosen perturbation threshold ε. This showcases a potential problem with the use of point-wise measures during training. The binary separation of "small" and "large" perturbations based on the perturbation threshold is not sufficient to capture the intricacies of human perception under perturbations, but a simplification based on the idea that perturbations below the perturbation threshold should almost certainly not lead to a change in classification. If a training procedure moves decision boundaries so that data points lie just beyond this threshold, it may achieve a low robust error, without furthering the actual goals of adversarial robustness research. Using robustness curves for evaluation cannot prevent this effect, but can be used to detect it.

3.2.3 Transfer of robustness across distance functions

In the following, we analyze to which extent properties of robustness curves transfer across different choices of distance

Table 1: Three point-wise measures for different threat models. All threat models use the ℓ_∞ distance function, but differ in choice of perturbation threshold (denoted by ε). Each row contains the robust test errors for one point-wise measure. Each column contains the robust test errors for one model, trained with a specific training method (marked by column title). The lower the number, the better the robustness for the specific threat model. Each point-wise measure results in a different relative ordering of the classifiers based on the errors. The order is visualized by different tones of gray in the background of the cells.

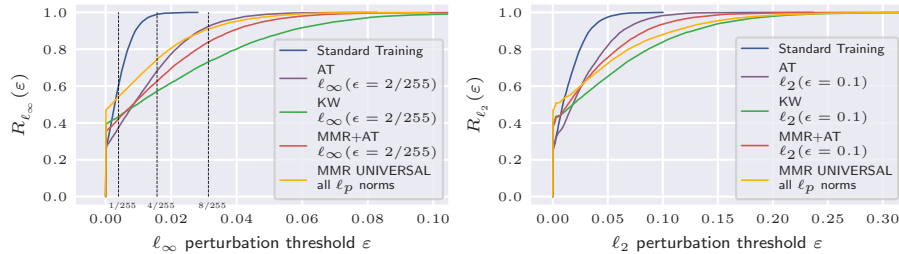| ε	ST	AT	KW	MMR + AT	MMR-UNIV
1/255	0.60	0.38	0.43	0.42	0.54
4/255	0.99	0.68	0.57	0.63	0.74
8/255	1.00	0.92	0.73	0.84	0.91

Figure 2: ℓ_∞ robustness curves (left plot) and ℓ_2 robustness curves (right plot) resulting from different training methods (indicated by label), optimized for different threat models (indicated by label). The dashed vertical lines visualize the three point-wise measures from Table 1. The models are trained and evaluated on the full training-/test sets of CIFAR-10. The curves allow us to reliably compare the robustness of the classifiers, unbiased by choice of perturbation threshold.

functions. If properties transfer, it may not be necessary to individually analyze robustness for each distance function.

In Figure 4 we compare the robustness of different models for the ℓ_∞ (left plot) and ℓ_2 (right plot) distance functions. The difference to Figure 2 is that the models (indicated by colour) are the same models in the left plot and in the right plot. We find that for MMR + AT, the ℓ_∞ threat model leads to better robustness than the ℓ_2 threat model *both* for ℓ_∞ *and* ℓ_2 robustness curves. In fact, MMR + AT with the ℓ_∞ threat model even leads to better ℓ_∞ and ℓ_2 robustness curves than MMR-UNIV, which is specifically designed to improve robustness for all ℓ_p norms. Overall, the plots are visually similar. However, since both plots contain multiple robustness curve intersections, the ranking of methods remains sensitive to the choice of perturbation threshold. For example, a perturbation threshold of $\varepsilon = 3/255$ (vertical black dashed line) for the ℓ_∞ distance function (left subplot) shows that the classifier trained with MMR + AT ($\ell_2(\varepsilon = 0.1)$) is approximately as robust as the classifier trained with MMR-UNIV. The same perturbation threshold for the ℓ_2 distance function (right subplot) shows that the classifier trained with MMR + AT is more robust than the classifier trained with MMR-UNIV for ℓ_2 threat models. Using typical perturbation thresholds from the literature for each distance function does not alleviate this issue: At perturbation threshold $\varepsilon = 2/255$ for ℓ_∞ distance, the classifier trained with MMR + AT ($\ell_2(\varepsilon = 0.1)$) is more robust than the one trained with MMR-UNIV, while at perturbation threshold $\varepsilon = 0.1$ for ℓ_2 distance, the opposite is true. This shows that even when robustness curves across various distance functions are qualitatively similar, this may be obscured by the choice of threat model(s) to compare on.

We also emphasize that in general, robustness curves across various distance functions may be qualitatively *dis*similar. In particular:

1. For linear classifiers, the *shape* of a robustness curve is identical for distances induced by different ℓ_p norms. This follows from Theorem 2 in Appendix B, which is an extension of a weaker result in Göpfert et al. [12]. For non-linear classifiers, different ℓ_p norms may induce different robustness curve shapes. See Göpfert et al. [12] for an example.
2. Even for linear classifiers, robustness curve *intersections* do not transfer between distances induced by different ℓ_p norms. That is, for two linear classifiers, there may exist p, p' such that the robustness curves for the ℓ_p distance intersect, but not the robustness curves for the $\ell_{p'}$ distance. See Appendix A for an example.

3.3 On the relationship between scale and data

As the previous sections show, robustness curves can be used to reveal properties of robust models that may be obscured by point-wise measures. However, some concept of scale, that is, some way to judge whether a perturbation is small or large, remains necessary. *Especially* when robustness curves intersect, it is crucial to be able to judge how critical it is for a model to be stable under the given perturbations. For many pairs of distance function and data set, canonical perturbation thresholds have emerged in the literature, but to the best of our knowledge, no reasons for these choices are given.

Since the assumption behind adversarial examples is that small perturbations should not affect classification behavior, the question of scale cannot be answered independently of the data
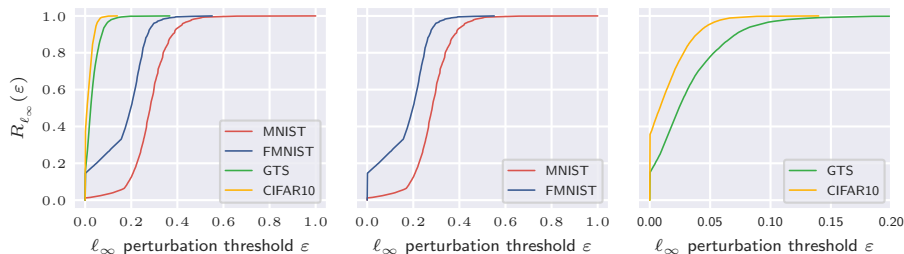
Figure 3: ℓ_∞ robustness curves for multiple data sets. Each curve is calculated for a different model and a different test data set. The data sets are indicated by the labels. The models are trained with `MMR + AT`, Threat Models: `MNIST`: $\ell_\infty(\varepsilon = 0.1)$, `FMNIST`: $\ell_\infty(\varepsilon = 0.1)$, `GTS`: $\ell_\infty(\varepsilon = 4/255)$, `CIFAR-10`: $\ell_\infty(\varepsilon = 2/255)$. The curves for `MNIST` and `FMNIST` both show a change in slope, which can not be captured with point-wise measures and could be a sign of overfitting to the specific threat models for which the classifiers were optimized for.
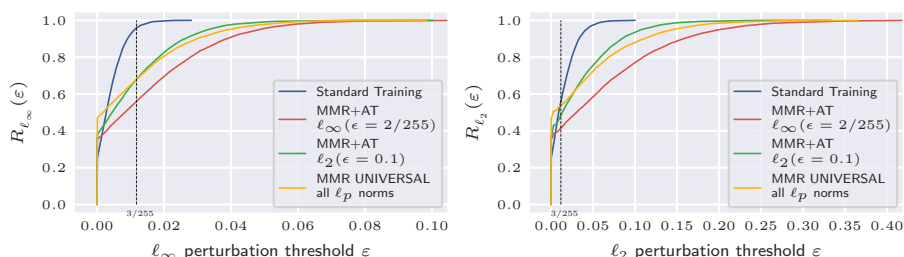

Figure 4: ℓ_∞ robustness curves (left plot) and ℓ_2 robustness curves (right plot) resulting from different training methods (indicated by color and label), optimized for different threat models (indicated by label). The models are trained and evaluated on the full training-/test sets of `CIFAR-10`. The curves allow us to reliably compare the transfer of robustness of the classifiers across distance functions, unbiased by choice of threat model.

distribution. In order to understand how to interpret different perturbation sizes, it can be helpful to understand how strongly the data point would need to be perturbed to *actually* change the *correct* classification. We call this the *inter-class distance* and analyze the distribution of inter-class distances for several popular data sets.

In Figure 5 we compare the inter-class distance distributions in ℓ_∞, ℓ_2, and ℓ_1 norm for all data sets considered in this work. We observe that for the ℓ_1 and ℓ_2 norms, the shape of the curves is similar across data sets, but their extent is determined by the dimensionality of the data space. In the ℓ_∞ norm, vastly different curves emerge for the different data sets. We hypothesize that, because the inter-class distance distributions vary more strongly for ℓ_∞ distances than for ℓ_1 distances, the results of robustifying a model w. r. t. ℓ_∞ distances may depend more strongly on the underlying data distribution than the results of robustifying w. r. t. ℓ_1 distances. This is an interesting avenue for future work.

When we look at the smallest inter-class distances in the ℓ_∞ norm (where all distances lie in the interval $[0, 1]$), we can make several observations. Because the smallest inter-class distance for `MNIST` in the ℓ_∞ norm is around 0.9, we can see that transforming an input from one class to one from a different class almost always requires completely flipping at least one pixel from almost-black to almost-white or vice versa. For the other datasets, the inter-class distance distributions are more spread out than the inter-class distance distribution of `MNIST`. We observe that for `CIFAR-10` with ℓ_∞ perturbations of size $\geqslant 0.25$,

it becomes possible to transform samples from different classes into each other, so starting from this threshold, any classifier must necessarily trade off between accuracy and robustness. The shapes of the curves and the threshold from which any classifier must necessarily trade of between accuracy and robustness differ strongly between data sets – refer to Table 2 for exact values for the threshold.

In Table 2, we summarize the smallest and largest inter-class distances in different norms together with additional information about the size, number of classes, and dimensionality of the all the data sets we consider in this work. The values correspond directly to Figure 5, but even in this simplified view, we can quickly make out key differences between the data sets. Compare, for example, `MNIST` and `GTS`: While it appears reasonable to expect ℓ_∞ robustness of 0.3 for `MNIST`, the same threshold for `GTS` is not possible. Relating Table 2 and Figure 3, we find entirely plausible the strong robustness results for `MNIST`, and the small perturbation threshold for `GTS`. Based on inter-class distances we also expect less ℓ_∞ robustness for `CIFAR-10` than for `FMNIST`, but not as seen in Figure 3. In any case, it is safe to say that, when judging the robustness of a model by a certain threshold, that number must be set with respect to the distribution the model operates on.

Overall, the strong dependence of robustness curves on the data set and the chosen norm, emphasizes the necessity of informed and conscious decisions regarding robustness thresholds. We
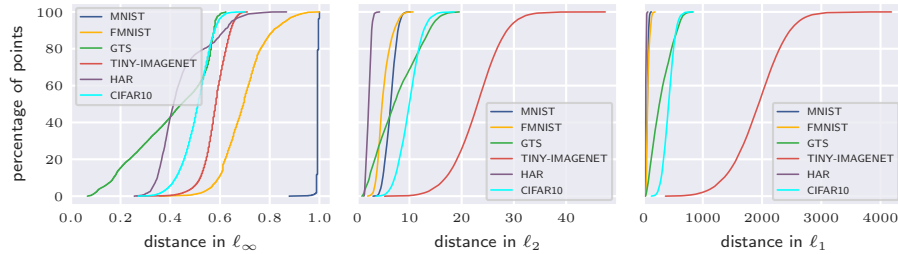
Figure 5: Minimum inter-class distances of all data sets considered in this work, measured in ℓ_∞ (left), ℓ_2 (middle), and ℓ_1 (right) norm. See Table 2 for size and dimensionality. The shapes of the curves and the threshold from which any classifier must necessarily trade of between accuracy and robustness differ strongly between data sets.

Table 2: Smallest and largest inter-class distances for subsets of several data sets, measured in l_∞, l_2, and l_1 norm, together with basic contextual information about the data sets. All data has been been normalized to lie within the interval [0, 1], and duplicates and corrupted data points have been removed. Apart from HAR, all data sets contain images – the dimensionality reported specifies their sizes and number of channels.

| | | | | Inter-class Distance | | | | | |
| | | | | Smallest | | | Largest | | |
Dataset	Samples	Classes	Dimensionality	l_∞	l_2	l_1	l_∞	l_2	l_1
MNIST	10 000	10	$28 \times 28 \times 1$	0.88	3.03	19.16	1.00	10.18	132.38
TINY-IMG	98 139	200	$64 \times 64 \times 3$	0.27	5.24	369.29	0.71	47.49	4184.37
FMNIST	10 000	10	$28 \times 28 \times 1$	0.36	2.00	24.87	1.00	10.70	194.29
GTS	10 000	43	$32 \times 32 \times 3$	0.07	0.90	31.46	0.62	19.54	833.22
CIFAR-10	10 000	10	$32 \times 32 \times 3$	0.27	3.61	130.77	0.70	18.57	831.44
HAR	2947	6	561	0.26	1.26	12.95	0.87	4.29	73.19

provide an easily accessible reference in the form of Table 2, that should prove useful while judging scales in a threat model.

4 Discussion

We have demonstrated that comparisons of robustness of different classifiers using point-wise measures can be heavily biased by the choice of perturbation threshold and distance function of the threat model, and that conclusions about rankings of classifiers with regards to their robustness based on point-wise measures therefore only provide a narrow view of the actual robustness behavior of the classifiers. Further, we have demonstrated different ways of using robustness curves to overcome the shortcomings of point-wise measures, and therefore recommend using them as the standard tool for comparing the robustness of classifiers. Finally, we have demonstrated how suitable perturbation thresholds necessarily depend on the data they pertain to.

It is our hope that practitioners and researchers alike will use the methodology proposed in this work, especially when developing and comparing adversarial defenses, and carefully motivate any concrete threat models they might choose, taking into account all available context.

Limitations: Computing approximate robustness curves for state-of-the-art classifiers and large data sets is computationally very intensive, due to the need of computing approximate minimal adversarial perturbations with strong adversarial attacks. Developing adversarial attacks which are both strong and fast is

an ongoing challenge in the field of adversarial robustness. Another limitation of our work is the focus on a small group of distance functions (mainly ℓ_∞ and ℓ_2 norms). Even though it does intuitively make sense that models should at least be robust against these types of perturbations, a more general evaluation able to consider more distance functions simultaneously could be advantageous.

References

[1] Jean-Baptiste Alayrac, Jonathan Uesato, Po-Sen Huang, Alhussein Fawzi, Robert Stanforth, and Pushmeet Kohli. "Are Labels Required for Improving Adversarial Robustness?" In: *Advances in Neural Information Processing Systems 32*. 2019, pp. 12214–12223.

[2] Davide Anguita, Alessandro Ghio, Luca Oneto, Xavier Parra, and J Reyes-Ortiz. "A Public Domain Dataset for Human Activity Recognition using Smartphones". In: *ESANN*. Jan. 2013.

[3] Akhilan Boopathy, Sijia Liu, Gaoyuan Zhang, Cynthia Liu, Pin-Yu Chen, Shiyu Chang, and Luca Daniel. "Proper Network Interpretability Helps Adversarial Robustness in Classification". en. In: *Proceedings of the International Conference on Machine Learning* 1 (2020).

[4] Wieland Brendel, Jonas Rauber, Matthias Kümmerer, Ivan Ustyuzhaninov, and Matthias Bethge. "Accurate, reliable and fast robustness evaluation". In: *Advances in Neural Information Processing Systems 32*. 2019, pp. 12861–12871.

[5]   Nicholas Carlini and David A. Wagner. "Towards Evaluating the Robustness of Neural Networks". In: *2017 IEEE Symposium on Security and Privacy (SP)*. 2017. arXiv: 1608.04644.

[6]   Nicholas Carlini et al. *On Evaluating Adversarial Robustness*. 2019. arXiv: 1902.06705.

[7]   Yair Carmon, Aditi Raghunathan, Ludwig Schmidt, Percy Liang, and John C. Duchi. *Unlabeled Data Improves Adversarial Robustness*. 2019. arXiv: 1905.13736.

[8]   Jeremy Cohen, Elan Rosenfeld, and Zico Kolter. "Certified Adversarial Robustness via Randomized Smoothing". In: *Proceedings of the 36th International Conference on Machine Learning, ICML*. Vol. 97. 2019, pp. 1310–1320.

[9]   Francesco Croce, Maksym Andriushchenko, and Matthias Hein. "Provable Robustness of ReLU networks via Maximization of Linear Regions". In: *Proceedings of Machine Learning Research*. 2019. arXiv: 1810.07481.

[10]   Francesco Croce and Matthias Hein. "Provable robustness against all adversarial l_p-perturbations for $p \geqslant 1$". In: *International Conference on Learning Representations*. 2020. arXiv: 1905.11213.

[11]   Ian J. Goodfellow, Jonathon Shlens, and Christian Szegedy. "Explaining and Harnessing Adversarial Examples". In: *3rd International Conference on Learning Representations*. 2015. arXiv: 1412.6572.

[12]   Christina Göpfert, Jan Philip Göpfert, and Barbara Hammer. "Adversarial Robustness Curves". In: *Machine Learning and Knowledge Discovery in Databases*. 2020. arXiv: 1908.00096.

[13]   Jan Philip Göpfert, André Artelt, Heiko Wersing, and Barbara Hammer. "Adversarial attacks hidden in plain sight". In: *Symposium on Intelligent Data Analysis*. 2020. arXiv: 1902.09286.

[14]   Chuan Guo, Mayank Rana, Moustapha Cisse, and Laurens van der Maaten. *Countering Adversarial Images using Input Transformations*. 2017. arXiv: 1711.00117.

[15]   Matthias Hein and Maksym Andriushchenko. *Formal Guarantees on the Robustness of a Classifier against Adversarial Manipulation*. 2017. arXiv: 1705.08475.

[16]   Dan Hendrycks, Mantas Mazeika, Saurav Kadavath, and Dawn Song. "Using Self-Supervised Learning Can Improve Model Robustness and Uncertainty". In: *Advances in Neural Information Processing Systems 32*. 2019, pp. 15663–15674. arXiv: 1901.09960.

[17]   Sebastian Houben, Johannes Stallkamp, Jan Salmen, Marc Schlipsing, and Christian Igel. "Detection of Traffic Signs in Real-World Images: The German Traffic Sign Detection Benchmark". In: *IJCNN*. 1288. 2013.

[18]   Diederik P. Kingma and Jimmy Ba. *Adam: A Method for Stochastic Optimization*. 2014. arXiv: 1412.6980.

[19]   Alex Krizhevsky. *Learning multiple layers of features from tiny images*. Tech. rep. 2009.

[20]   M. Lecuyer, V. Atlidakis, R. Geambasu, D. Hsu, and S. Jana. "Certified Robustness to Adversarial Examples with Differential Privacy". In: *2019 IEEE Symposium on Security and Privacy (SP)*. 2019, pp. 656–672. arXiv: 1802.03471.

[21]   Guang-He Lee, Yang Yuan, Shiyu Chang, and Tommi Jaakkola. "Tight Certificates of Adversarial Robustness for Randomly Smoothed Classifiers". In: *Advances in Neural Information Processing Systems 32*. 2019, pp. 4910–4921.

[22]   Bai Li, Changyou Chen, Wenlin Wang, and Lawrence Carin. "Certified Adversarial Robustness with Additive Noise". In: *Advances in Neural Information Processing Systems 32*. 2019, pp. 9464–9474.

[23]   Fei-Fei Li, Andrej Karpathy, and Justin Johnson. *CS231n: Convolutional Neural Networks for Visual Recognition*. [Online; accessed March 28, 2020]. 2016. URL: http://cs231n.stanford.edu/2016/project.html.

[24]   Aleksander Madry, Aleksandar Makelov, Ludwig Schmidt, Dimitris Tsipras, and Adrian Vladu. "Towards Deep Learning Models Resistant to Adversarial Attacks". In: *ICLR*. 2018. arXiv: 1706.06083.

[25]   Saeed Mahloujifar, Xiao Zhang, Mohammad Mahmoody, and David Evans. "Empirically Measuring Concentration: Fundamental Limits on Intrinsic Robustness". In: *Advances in Neural Information Processing Systems 32*. 2019, pp. 5209–5220.

[26]   Pratyush Maini, Eric Wong, and Zico Kolter. "Adversarial Robustness Against the Union of Multiple Threat Models". en. In: *Proceedings of the International Conference on Machine Learning* 1 (2020).

[27]   Chengzhi Mao, Ziyuan Zhong, Junfeng Yang, Carl Vondrick, and Baishakhi Ray. "Metric Learning for Adversarial Robustness". In: *Advances in Neural Information Processing Systems 32*. 2019, pp. 480–491. arXiv: 1909.00900.

[28]   Amir Najafi, Shin-ichi Maeda, Masanori Koyama, and Takeru Miyato. "Robustness to Adversarial Perturbations in Learning from Incomplete Data". In: *Advances in Neural Information Processing Systems 32*. 2019, pp. 5541–5551.

[29]   Rafael Pinot, Laurent Meunier, Alexandre Araujo, Hisashi Kashima, Florian Yger, Cedric Gouy-Pailler, and Jamal Atif. "Theoretical evidence for adversarial robustness through randomization". In: *Advances in Neural Information Processing Systems 32*. 2019, pp. 11838–11848.

[30]   Chongli Qin et al. "Adversarial Robustness through Local Linearization". In: *Advances in Neural Information Processing Systems 32*. 2019, pp. 13847–13856.

[31]   Jonas Rauber, Wieland Brendel, and Matthias Bethge. *Foolbox: A Python toolbox to benchmark the robustness of machine learning models*. 2017. arXiv: 1707.04131.

[32]   Leslie Rice, Eric Wong, and Zico Kolter. "Overfitting in adversarially robust deep learning". en. In: *Proceedings of the International Conference on Machine Learning* 1 (2020).

[33]   Sahil Singla and Soheil Feizi. "Second-Order Provable Defenses against Adversarial Attacks". en. In: *Proceedings of the International Conference on Machine Learning* 1 (2020).

[34]   Chuanbiao Song, Kun He, Jiadong Lin, Liwei Wang, and John E. Hopcroft. "Robust Local Features for Improving the Generalization of Adversarial Training". en. In: Apr. 2020.

[35]   Christian Szegedy, Wojciech Zaremba, Ilya Sutskever, Joan Bruna, Dumitru Erhan, Ian J. Goodfellow, and Rob Fergus. *Intriguing properties of neural networks*. 2014. arXiv: 1312.6199.

[36]   Florian Tramer and Dan Boneh. "Adversarial Training and Robustness for Multiple Perturbations". In: *Advances in Neural Information Processing Systems 32*. 2019, pp. 5866–5876.

[37]   Yisen Wang, Difan Zou, Jinfeng Yi, James Bailey, Xingjun Ma, and Quanquan Gu. "Improving Adversarial Robustness Requires Revisiting Misclassified Examples". en. In: Apr. 2020.

[38]   Eric Wong and Zico Kolter. "Provable Defenses against Adversarial Examples via the Convex Outer Adversarial Polytope". In: *Proceedings of the 35th International Conference on Machine Learning*. 2018. arXiv: 1711.00851.

[39]   Eric Wong, Leslie Rice, and J. Zico Kolter. "Fast is better than free: Revisiting adversarial training". en. In: Apr. 2020.

[40] Eric Wong, Frank R. Schmidt, and J. Zico Kolter. "Wasserstein Adversarial Examples via Projected Sinkhorn Iterations". In: *Proceedings of the 36th International Conference on Machine Learning, ICML*. Vol. 97. Proceedings of Machine Learning Research. 2019, pp. 6808–6817.

[41] Han Xiao, Kashif Rasul, and Roland Vollgraf. *Fashion-MNIST: a Novel Image Dataset for Benchmarking Machine Learning Algorithms*. 2017. arXiv: 1708.07747.

[42] Cihang Xie and Alan Yuille. "Intriguing Properties of Adversarial Training at Scale". en. In: Apr. 2020.

[43] Jingfeng Zhang, Xilie Xu, Bo Han, Gang Niu, Lizhen Cui, Masashi Sugiyama, and Mohan Kankanhalli. "Attacks Which Do Not Kill Training Make Adversarial Learning Stronger". en. In: *Proceedings of the International Conference on Machine Learning* 1 (2020).

A ROBUSTNESS CURVES WITH ARBITRARY INTERSECTIONS

Theorem 1. *Let* $T_1, T_2 \subset \mathbb{R}^{>0}$ *be two disjoint finite sets. Then there exists a distribution P on $\mathbb{R} \times \{0,1\}$ and two classifiers $c_1, c_2 : \mathbb{R} \to \{0,1\}$ such that $R_{|\cdot|}^{c_1}(t) < R_{|\cdot|}^{c_2}(t)$ for all $t \in T_1$ and $R_{|\cdot|}^{c_1}(t) > R_{|\cdot|}^{c_2}(t)$ for all $t \in T_2$.*

Proof. Without loss of generality, assume that $T_1 = \{t_1, \ldots, t_n\}$ and $T_2 = \{t'_1, \ldots, t'_n\}$ with $t_i < t'_i < t_{i+1}$ for $i \in \{1, \ldots, n\}$. We will construct c_1, c_2 such that the robustness curves $R_{|\cdot|}^{c_1}(\cdot), R_{|\cdot|}^{c_2}(\cdot)$ intersect at exactly the points $(t_i + t'_i)/2$ and $(t_i + t'_{i+1})/2$ on the interval $(t_1, t'_n]$. Let $d = t'_n$ and

$$P\left(-d - \frac{t_i + t'_{i+1}}{2}, 0\right) = P\left(d + \frac{t_i + t'_i}{2}, 1\right) = \frac{2}{4n+1}$$

and

$$P\left(-d - \frac{t_1}{2}, 0\right) = \frac{1}{4n+1}.$$

Let $c_1(x) = \mathbb{1}_{x \geqslant -d}$ and $c_2(x) = \mathbb{1}_{x \geqslant d}$. Both classifiers have perfect accuracy on P, meaning that $R_{|\cdot|}^{c_i}(0) = 0$. The closest point to the decision boundary of c_1 is $-d - \frac{t_1}{2}$ with weight $\frac{1}{4n+1}$, so $R_{|\cdot|}^{c_1}(\frac{t_1}{2}) = \frac{1}{4n+1}$. The second-closest point is $-d - \frac{t_1 + t'_2}{2}$ with weight $\frac{2}{4n+1}$, so $R_{|\cdot|}^{c_1}(\frac{t_1 + t'_2}{2}) = \frac{3}{4n+1}$, and so on. Meanwhile, the closest point to the decision boundary of c_2 is $d + \frac{t_1 + t'_1}{2}$ with weight $\frac{2}{4n+1}$, so $R_{|\cdot|}^{c_2}(\frac{t_1 + t'_1}{2}) = \frac{2}{4n+1}$, the second-closest point is $d \frac{t_2 + t'_2}{2}$ with weight $\frac{2}{4n+1}$, so $R_{|\cdot|}^{c_2}(\frac{t_2 + t'_2}{2}) = \frac{4}{4n+1}$, and so on. $\square$

Example 1. *To see that robustness curve intersections do not transfer between different ℓ_p norms, consider the example in Figure 6. The blue and orange linear classifiers both perfectly separate the displayed data. The ℓ_∞ robustness curves of the classifiers do not intersect, meaning that the robust error of the blue classifier is always better than that of the orange classifier. In ℓ_2 distance, the robustness curves intersect, so that there is a range of perturbation sizes where the orange classifier has better robust error than the blue classifier.*

B ROBUSTNESS CURVE DEPENDENCE OF SHAPE ON DISTANCE FUNCTION

Theorem 2. *Let $f(x) = \operatorname{sgn}(w^T x + b)$ be a linear classifier. Then the* shape *of the robustness curve for f regarding an ℓ_p norm-induced distance does not depend on the choice of p. It holds that*

$$R_{\ell_{p_1}}^f(\varepsilon) = R_{\ell_{p_2}}^f(c \cdot \varepsilon) \quad \forall \, \varepsilon \text{ for } c = \frac{\|w\|_{q_1}}{\|w\|_{q_2}}, q_i = \frac{p_i}{p_i - 1}. \quad (1)$$

Lemma 1. *Let $x \in \mathbb{R}^m$ with $w^T x + b \neq 0$. Let $p \in [1, \infty]$ and q such that $\frac{1}{p} + \frac{1}{q} = 1$, where we take $\frac{1}{\infty} = 0$. Then*

$$\min\{\|\delta\|_p : \operatorname{sgn}(w^T(x + \delta) + b) \neq \operatorname{sgn}(w^T x + b)\} = \frac{|w^T + b|}{\|w\|_q} \quad (2)$$

and the minimum is attained by

$$\delta = \begin{cases} \frac{-w^T x - b}{\|w\|_\infty} \operatorname{sgn}(w_j) e_j, j = \operatorname{argmax}_i |w_i| & p = 1 \\ \frac{-w^T x - b}{\|w\|_q^q} (\operatorname{sgn}(w_i)|w_i|^{\frac{1}{p-1}})_{i=1}^d & p \in (1, \infty]. \end{cases} \quad (3)$$

where $x^{\frac{1}{\infty-1}} = x^0 = 1$ and e_j is the j-th unit vector.

Proof of Theorem 2. By Hölder's inequality, for any δ,

$$\sum_{i=1}^m |w_i \delta_i| \leqslant \|\delta\|_p \|w\|_q. \quad (4)$$

For δ such that $\operatorname{sgn}(w^T(x + \delta) + b) \neq \operatorname{sgn}(w^T x + b)$ it follows that

$$\|\delta\|_p \geqslant \frac{\sum_{i=1}^m |w_i \delta_i|}{\|w\|_q} \geqslant \frac{|\sum_{i=1}^m w_i \delta_i|}{\|w\|_q} \geqslant \frac{|w^T x + b|}{\|w\|^q}. \quad (5)$$

Using the identity $q = \frac{p}{p-1}$, it is easy to check that for every $p \in [1, \infty]$, with δ as defined in Equation (3),

1. $w^T \delta = -w^T x - b$, so that $w^T(x + \delta) + b = 0$, and

2. $\|\delta\|_p = \frac{|w^T x + b|}{\|w\|_q}$.

Item 1 shows that δ is a feasible point, while Item 2 in combination with **??** shows that $\|\delta\|_p$ is minimal. $\square$

Using Lemma 1, we are ready to prove Theorem 2.

Proof. By definition,

$$R_{\ell_{p_1}}^f(\varepsilon) = P(\underbrace{\{(x,y) \text{ s.t. } \exists \, \delta : \|\delta\|_{p_1} \leqslant \varepsilon \wedge f(x + \delta) \neq y\}}_{\mathcal{R}_{p_1}(\varepsilon)}). \quad (6)$$

We can split $\mathcal{R}_{p_1}(\varepsilon)$ into the disjoint sets

$$\underbrace{\{(x,y) : f(x) \neq y\}}_{=M} \quad (7)$$

$$\dot{\cup} \quad (8)$$

$$\underbrace{\{(x,y) \text{ s.t. } \exists \, \delta : \|\delta\|_{p_1} \leqslant \varepsilon \wedge y = f(x) \neq f(x + \delta)\}}_{=B_{p_1}(\varepsilon)}. \quad (9)$$
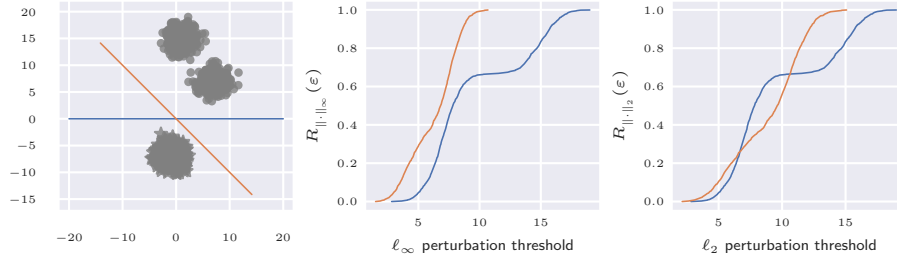
Figure 6: Example of a data distribution and two linear classifiers such that the ℓ_2 robustness curves intersect, but not the ℓ_∞ robustness curves.

Choose q_1, q_2 such that $\frac{1}{p_i} + \frac{1}{q_i} = 1$. By Lemma 1, and using that $f(x) = \text{sgn}(w^T x + b)$,

$$B_{p_1}(\varepsilon) = \{(x, y) : \text{sgn}(w^T x + b) = y \wedge \frac{|w^T x + b|}{\|w\|_{q_1}} \leqslant \varepsilon\} \quad (10)$$

$$= \{(x, y) : \text{sgn}(w^T x + b) = y \wedge \frac{|w^T x + b|}{\|w\|_{q_2}} \leqslant \frac{\|w\|_{q_1}}{\|w\|_{q_2}} \varepsilon\}) \quad (11)$$

$$= B_{p_2}\left(\frac{\|w\|_{q_1}}{\|w\|_{q_2}} \varepsilon\right). \quad (12)$$

This shows that

$$R^f_{\ell_{p_1}}(\varepsilon) = P(M) + P(B_{p_1}(\varepsilon)) \quad (13)$$

$$= P(M) + P\left(B_{p_2}\left(\frac{\|w\|_{q_1}}{\|w\|_{q_2}} \varepsilon\right)\right) \quad (14)$$

$$= R^f_{\ell_{p_2}}\left(\frac{\|w\|_{q_1}}{\|w\|_{q_2}} \varepsilon\right). \quad (15)$$

$\square$

C EXPERIMENTAL DETAILS

C.1 Model training

We use the same model architecture as Croce et al. [9] and Wong and Kolter [38]. Unless explicitly stated otherwise, the trained models are taken from Croce et al. [9]. The exact architecture of the model is: Convolutional layer (number of filters: 16, size: 4x4, stride: 2), ReLu activation function, convolutional layer (number of filters: 32, size: 4x4, stride: 2), ReLu activation function, fully connected layer (number of units: 100), ReLu activation function, output layer (number of units depends on the number of classes). All models are trained with Adam Optimizer [18] for 100 epochs, with batch size 128 and a default learning rate of 0.001. More information on the training can be found in the experimental details section of the appendix of Croce et al. [9]. The trained models are those made publicly available by Croce et al. [9][5]and Croce and Hein [10][6].

C.2 Approximated robustness curves

We use state-of-the-art adversarial attacks to approximate the true minimal distances of input datapoints to the decision boundary of a classifier for our adversarial robustness curves (see Definition 1). We base our selection of attacks on the recommendations of Carlini et al. [6]. Specifically, we use the following attacks: For ℓ_2 robustness curves we use the ℓ_2-attack proposed by Carlini and Wagner [5] and for ℓ_∞ robustness curves we use PGD [24]. For both attacks, we use the implementations of Foolbox [31]. For the ℓ_∞ attack, we use the standard hyperparameters of the Foolbox implementation. For the ℓ_1 and ℓ_2 attacks we increase the number of binary search steps that are used to find the optimal tradeoff-constant between distance and confidence from 5 to 10, which we found empirically to improve the results. For the rest of the hyperparameters, we again use the standard values of the Foolbox implementation.

C.3 Computational architecture

We executed all programs on an architecture with 2 x Intel Xeon(R) CPU E5-2640 v4 @ 2.4 GHz, 2 x Nvidia GeForce GTX 1080 TI 12G and 128 GB RAM.

---

[5]The models trained with ST, KW, AT and MMR + AT are avaible at www.github.com/max-andr/provable-robustness-max-linear-regions.

[6]The models trained with MMR-UNIV are avaible at www.github.com/fra31/mmr-universal.